Multi-phase compressible compositional simulations with phase equilibrium computation in the VTN specification *

Tomáš Smejkal[1[0000−0003−4331−5160]] and Jiří Mikyška[1[0000−0001−6017−2259]]

Czech Technical University in Prague, Faculty of Nuclear Sciences and Physical Engineering, Department of Mathematics, Trojanova 13, 120 00 Prague 2, Czech Republic tomas.smejkal@fjfi.cvut.cz

Abstract. In this paper, we present a numerical solution of a multi-phase compressible Darcy's flow of a multi-component mixture in a porous medium. The mathematical model consists of mass conservation equation of each component, extended Darcy's law for each phase, and an appropriate set of the initial and boundary conditions. The phase split is computed using the phase equilibrium computation in the VTN-specification (known as VTN-flash). The transport equations are solved numerically using the mixed-hybrid finite element method and a novel iterative IMPEC scheme [1]. We provide two examples showing the performance of the numerical scheme.

Keywords: Compositional simulations · Multi-phase flow · Phase equilibrium computation · Mixed-hybrid finite element method · VTN-flash · VTN-stability · Iterative IMPEC · Darcy's flow.

1 Introduction

The mathematical modeling of compositional flow in a porous medium is an important topic in chemical engineering and has many applications in the industry, e.g., CO_2 sequestration or enhanced oil recovery. The mathematical model has to include a transport equation for each component in the mixture and a thermodynamical model describing the local equilibrium behavior.

In literature, two main approaches for solving the transport equations are common. The first approach, known as IMPEC [2], solves the equations in two

* The work was supported by the project Development and application of advanced methods for mathematical modeling of natural and industrial processes using high-performance computing, project no. SGS20/184/OHK4/3T/14 of the Student Grant Agency of the Czech Technical University in Prague, 2020-2022, the project Multiphase flow, transport, and structural changes related to water freezing and thawing in the subsurface of the Czech Science Foundation, project no. 21-09093S, and the project Center for advanced applied science, project no. CZ.02.1.01/0.0/0.0/16-019/0000778, supported by the Operational Programme Research, Development and Education, co-financed by the European Structural and Investment Funds and the state budget of the Czech Republic, 2018-2023.

ICCS Camera Ready Version 2021
To cite this paper please use the final published version:
DOI: 10.1007/978-3-030-77980-1_13

steps. First, the pressure equation is solved implicitly to get the pressure field. Then, the concentrations of the first $n-1$ components are updated explicitly using the pressure from the previous step. The concentration of the last component is updated using the previous ones, the total concentration, and the equation of state. The conservation of mass holds for the $n-1$ components. However, for the last n-th component, the conservation of mass does not hold [1]. Chen et al. [1] presented a novel iterative IMPEC scheme where the conservation of mass of all components is guaranteed. An alternative to the IMPEC approach is the one of Young and Stephenson [3], where a method based on the Newton-Raphson iterations is used.

Concerning the thermodynamical model, traditionally, the PTN approach (constant pressure, temperature, and moles) [4, 5] is used to determine the composition of equilibrium phases. No matter how wide-spread the PTN-specification is, the approach has some limitations [6, 7], e.g., the equilibrium state of the system is not always determined uniquely. Alternatively, the VTN approach (constant volume, temperature, and moles) [6, 8, 9] can be used to determine the equilibrium state. Since most equations of state are given explicitly in pressure, i.e., $p = p(T, V, N_1, \ldots, N_n)$, the VTN-approach has some benefits, e.g., the inversion of the equation of state does not have be performed, and the equilibrium states are uniquely determined.

In this work, we are interested in modeling of the compositional flow with the use of the phase equilibrium computation. One approach, is using the IMPEC method with PTN approach, e.g., [10–12]. Alternatively, the VTN approach can be used. In our previous work [7], we use a fully implicit scheme, which gives the pressure field directly. However, this approach is computationally intensive. Therefore, we are proposing an alternative method based on the IMPEC strategy using the VTN-specification.

In this paper, we present a new numerical solution of the multi-phase compositional model. The solution is based on a novel iterative IMPEC scheme [1] that was originally developed for the single-phase compositional flow. In this paper, we extend this method to multi-phase problems. The stabilization of the numerical scheme is ensured by an upwind technique. The chemical equilibrium is computed locally on each finite element using the VTN-phase stability testing and VTN-phase equilibrium computation. In this approach, the Helmholtz free energy density of the system is minimized to obtain the equilibrium state. We are using the Newton-Raphson method with line-search and the modified Cholesky decomposition to find the minimum [8, 13].

The structure of this paper is as follows. In Section 2, the physical and mathematical model describing compressible multi-phase multi-component compositional flow will be presented. In Section 3, the numerical solution will be given. In Section 4, examples showing the performance will be presented. In Section 5, the results are discussed, and some conclusions are drawn.

ICCS Camera Ready Version 2021
To cite this paper please use the final published version:
DOI: 10.1007/978-3-030-77980-1_13

2 Physical and Mathematical model

2.1 Physical model

In this paper, the studied system is a fixed porous medium filled with a multi-component fluid. The porous medium in our interests are the hydrocarbon reservoirs. Based on the injection and the boundary condition, we study the flow of this multi-component multi-phase fluid through the fixed porous medium.

2.2 Transport equations

Consider a mixture of n components with a constant temperature T. The mass balance equation for component $i \in \widehat{n}$ (the symbol $\widehat{n}$ represents a set of positive integers not exceeding n) is

$$\frac{\partial(\phi c_i)}{\partial t} + \boldsymbol{\nabla} \cdot \mathbf{q}_i = f_i, \tag{1}$$

where ϕ [-] is the porosity, c_i [mol m^{-3}] is the molar concentration (density) of the i-th component, $\mathbf{q}_i$ [mol m^{-2} s^{-1}] is the flux of the i-th component, and f_i [mol m^{-3} s^{-1}] is the source/sink of the i-th component. For a multi-phase system without diffusion, the flux $\mathbf{q}_i$ can be expressed as

$$\mathbf{q}_i = \left(\sum_{\alpha=1}^{\Pi} c_{\alpha,i} \mathbf{u}_\alpha \right), \tag{2}$$

where $c_{\alpha,i}$ [mol m^{-3}] is the concentration of the i-th component in phase α, Π is the number of phases presented in the phase split, and $\mathbf{u}_\alpha$ [m s^{-1}] is the velocity of phase α. The relation between concentrations c_i and $c_{\alpha,i}$ is presented in Section 2.4. The velocity of each phase is model using Darcy's law

$$\mathbf{u}_\alpha = -\lambda_\alpha \mathbf{K} \left(\boldsymbol{\nabla} p - \rho_\alpha \mathbf{g} \right), \tag{3}$$

where λ_α [kg^{-1} m s] is the mobility of phase α, $\mathbf{K}$ [m^2] is the intrinsic permeability tensor, p [Pa] is the pressure, ρ_α [kg m^{-3}] is the mass density of phase α, and $\mathbf{g}$ [m s^{-2}] is the gravity acceleration. The mobility and the density are calculated using

$$\lambda_\alpha = \frac{k_{r\alpha}(S_\alpha)}{\eta_\alpha \left(T, c_{\alpha,1}, \ldots, c_{\alpha,n}\right)}, \quad \rho_\alpha = \sum_{i=1}^{n} c_{\alpha,i} M_i, \tag{4}$$

where $k_{r\alpha}$ [-] is the relative permeability, S_α [-] is the saturation, η_α [kg m^{-1} s^{-1}] is the dynamic viscosity, and M_i [kg mol^{-1}] is the molar weight of the i-th component. In this work, we are using a linear model to compute the relative permeability:

$$k_{r\alpha}(S_\alpha) = S_\alpha. \tag{5}$$

ICCS Camera Ready Version 2021
To cite this paper please use the final published version:
DOI: 10.1007/978-3-030-77980-1_13

The dynamic viscosity η_α is calculated using the Lohrenz, Bray and Clark model [14]. The mathematical model has to be supplemented with an equation which connects the concentrations and the pressure:

$$p = p^{(eq)}\left(c_1, \ldots, c_n\right). \tag{6}$$

Details are in Section 2.4. Using equation (6), the mass conservation (1), and the chain rule

$$\frac{\partial p}{\partial t} = \sum_{i=1}^{n} \frac{\partial p^{(eq)}}{\partial c_i} \frac{\partial c_i}{\partial t}, \tag{7}$$

the equation known-as pressure equation can be derived. In the VTN-formulation the pressure equation reads as

$$\phi \frac{\partial p}{\partial t} + \sum_{i=1}^{n} \Theta_i (\boldsymbol{\nabla} \cdot \mathbf{q}_i - f_i) = 0, \tag{8}$$

where $\Theta_i = \frac{\partial p^{(eq)}}{\partial c_i}$.

2.3 Fluxes definition

In this section, we define fluxes needed for the description of the numerical scheme. Let

$$\mathbf{q}_{\alpha,i} = c_{\alpha,i} \mathbf{u}_\alpha \tag{9}$$

be the flux of the i-component of phase α. Then, the flux of phase α is

$$\mathbf{q}_\alpha = \sum_{i=1}^{n} \mathbf{q}_{\alpha,i} = c_\alpha \mathbf{u}_\alpha, \tag{10}$$

where $c_\alpha = \sum_{i=1}^{n} c_{\alpha,i}$ is the total concentration of phase α. Lastly, the total flux $\mathbf{q}$ is defined as

$$\mathbf{q} = \sum_{\alpha=1}^{\Pi} \mathbf{q}_\alpha = \sum_{\alpha=1}^{\Pi} c_\alpha \mathbf{u}_\alpha, \tag{11}$$

and the total velocity $\mathbf{u}$ as

$$\mathbf{u} = \sum_{\alpha=1}^{\Pi} \mathbf{u}_\alpha. \tag{12}$$

Inserting equation (3) into previous equation results in

$$\mathbf{u} = -\lambda \mathbf{K} \left(\boldsymbol{\nabla} p - \rho^{(avg)} \mathbf{g} \right), \tag{13}$$

ICCS Camera Ready Version 2021
To cite this paper please use the final published version:
DOI: 10.1007/978-3-030-77980-1_13

where the total mobility λ and the average density $\rho^{(avg)}$ are defined as

$$\lambda = \sum_{\alpha=1}^{\Pi} \lambda_\alpha, \quad \rho^{(avg)} = \frac{\sum_{\alpha=1}^{\Pi} \lambda_\alpha \rho_\alpha}{\lambda}. \tag{14}$$

As the tensor $\mathbf{K}$ is positive definite, its inversion exists, and the gradient $\boldsymbol{\nabla} p$ can be expressed from equation (13) as

$$\boldsymbol{\nabla} p = -\lambda^{-1}\mathbf{K}^{-1}\mathbf{u} + \rho^{(avg)}\mathbf{g}. \tag{15}$$

Inserting previous equation into Darcy's law (3) results in

$$\mathbf{u}_\alpha = \lambda^{-1}\lambda_\alpha \left(\mathbf{u} - \sum_{\beta=1}^{\Pi} \lambda_\beta(\rho_\beta - \rho_\alpha)\mathbf{K}\mathbf{g} \right). \tag{16}$$

Therefore, the flux of the i-th component in phase α is

$$\mathbf{q}_{\alpha,i} = c_{\alpha,i}\lambda^{-1}\lambda_\alpha \left(\mathbf{u} - \sum_{\beta=1}^{\Pi} \lambda_\beta(\rho_\beta - \rho_\alpha)\mathbf{K}\mathbf{g} \right). \tag{17}$$

2.4 Phase stability testing and phase equilibrium calculation

Depending on the mixture's temperature and concentrations, the state can be in one or more phases. The phase stability testing [6] and phase equilibrium computation [8] is used to determine the number of phases and the composition of each phase described by $c_1, \ldots, c_n$ and T. In the VTN-phase stability testing the goal is to predict whether a given state is stable or if this state is unstable and splitting will occur. The VTN-phase equilibrium computation is used to determine the composition of the equilibrium state. The problem can be defined as an optimization task minimizing the objective function

$$a^{(\Pi)}\left(\mathbf{c}^{(1)}, \ldots, \mathbf{c}^{(\Pi)}, \mathbf{S}\right) = \sum_{\alpha=1}^{\Pi} S_\alpha a\left(c_{\alpha,1}, \ldots, c_{\alpha,n}\right) \tag{18}$$

subject to

$$\sum_{\alpha=1}^{\Pi} S_\alpha = 1, \quad \sum_{\alpha=1}^{\Pi} S_\alpha c_{\alpha,i} = c_i^*, \quad i \in \widehat{n}, \tag{19}$$

where a is the Helmholtz free energy density (for details see, e.g., [15, 16]), $\mathbf{S} = (S_1, \ldots, S_\Pi)^T$ and $\mathbf{c}^{(\alpha)} = (c_{\alpha,1}, \ldots, c_{\alpha,n})^T$ for $\alpha \in \widehat{\Pi}$. The necessary equilibrium conditions are [8]

$$p(c_{\alpha,1}, \ldots, c_{\alpha,n}) = p(c_{\beta,1}, \ldots, c_{\beta,n}), \quad \forall \alpha, \beta \in \widehat{\Pi}, \alpha \neq \beta, \tag{20}$$

$$\mu_i(c_{\alpha,1}, \ldots, c_{\alpha,n}) = \mu_i(c_{\beta,1}, \ldots, c_{\beta,n}), \quad \forall \alpha, \beta \in \widehat{\Pi}, \alpha \neq \beta, \forall i \in \widehat{n}, \tag{21}$$

ICCS Camera Ready Version 2021
To cite this paper please use the final published version:
DOI: 10.1007/978-3-030-77980-1_13

where μ_i is the chemical potential of the i-th component. If the state is in one phase ($\Pi = 1$), the equilibrium pressure $p^{(eq)}$ (6) is given by the equation of state

$$p^{(eq)}(c_1, \ldots, c_n) = p^{(EOS)}(c_1, \ldots, c_n). \tag{22}$$

In this work, we use the Peng-Robinson equation of state [17] in the following form

$$p^{(EOS)}(c_1, \ldots, c_n) = \frac{\sum_{i=1}^n c_i RT}{1 - \sum_{i=1}^n b_i c_i} - \frac{\sum_{i,j=1}^n a_{ij} c_i c_j}{1 + 2\sum_{i=1}^n b_i c_i - \left(\sum_{i=1}^n b_i c_i\right)^2}, \tag{23}$$

where a_{ij}, b_i are parameters. See [15, 17] for details. On the other hand, if the equilibrium state is in $\Pi > 1$ phases, the equilibrium pressure $p^{(eq)}$ is given by

$$p^{(eq)}(c_1, \ldots, c_n) = p^{(EOS)}(c_{\alpha,1}, \ldots, c_{\alpha,n}), \tag{24}$$

for an arbitrary $\alpha \in \widehat{\Pi}$ since the pressures of each phase in the phase equilibrium are equal (see equation (20)).

2.5 Initial and boundary conditions

Now, let us summarize the equations and define the initial and boundary conditions. Let $\Omega \subset \mathbb{R}^d$ is a bounded domain and J is a time interval. In $J \times \Omega$, we solve equations (1) and (8) for $p = p(t, \mathbf{x})$ and $c_i = c_i(t, \mathbf{x})$, $i \in \widehat{n}$. The fluxes $\mathbf{q}_i$ are given by equation (2), and the velocities $\mathbf{u}_\alpha$ are computed using Darcy's law (3). The composition of the multi-phase state is determined by solving the optimization problem given by (18) and (19). The mathematical model has to be equipped with initial conditions and an appropriate set of boundary conditions. The initial conditions read as

$$c_i(0, \mathbf{x}) = c_i^{(\text{ini})}, \quad \forall \mathbf{x} \in \Omega, \forall i \in \widehat{n}, \tag{25}$$

$$p(0, \mathbf{x}) = p^{(eq)}\left(c_1^{(\text{ini})}, \ldots, c_n^{(\text{ini})}\right), \quad \forall \mathbf{x} \in \Omega. \tag{26}$$

Moreover, we impose the following boundary conditions

$$p(t, \mathbf{x}) = p^{(D)}(t, \mathbf{x}), \mathbf{x} \in \Gamma_p, t \in J, \tag{27}$$

$$\mathbf{q}_i(t, \mathbf{x}) \cdot \mathbf{n}(\mathbf{x}) = 0, \mathbf{x} \in \Gamma_q, t \in J, \tag{28}$$

where $\mathbf{n}$ is the unit outward normal vector to the boundary $\partial\Omega, \Gamma_p \cup \Gamma_q = \partial\Omega$, and $\Gamma_p \cap \Gamma_q = \emptyset$.

3 Numerical solution

In this work, we assume that the computation domain Ω is a 2D rectangular domain. We use a triangulation $\tau_\Omega = \left\{K_i; i \in \widehat{N}_{el}\right\}$, where N_{El} is the number of elements. Moreover, we denote N_{Si} the number of sides.

ICCS Camera Ready Version 2021
To cite this paper please use the final published version:
DOI: 10.1007/978-3-030-77980-1_13

3.1 Disretization of Darcy's law

On each element $K \in \tau_\Omega$, we shall approximate $\mathbf{u}$ in the lowest order Raviar-Thomas space $\mathbf{RT}_0(K)$ [18, 19]

$$\mathbf{u}(t, \mathbf{x}) = \sum_{E \in \partial K} u_{K,E}(t) \mathbf{w}_{K,E}(\mathbf{x}), \tag{29}$$

where $\mathbf{w}_{K,E}$ are the basis functions and $u_{K,E}$ is the velocity across the side E in the outward direction with respect to K. Multiplying equation (15) with function $\mathbf{w}_{K,E'}$, integrating over element $K \in \tau_\Omega$, and using the Gauss-Ostrogradski theorem results in the weak formulation of Darcy's law

$$\widehat{p}_{K,E'} - p_K = -\lambda_K^{-1} \sum_{E \in \partial K} u_{K,E}(t) \int_K (\mathbf{K}^{-1} \mathbf{w}_{K,E}) \cdot \mathbf{w}_{K,E'} \mathrm{d}\mathbf{x} + \rho_K^{(avg)} \int_K \mathbf{g} \cdot \mathbf{w}_{K,E'} \mathrm{d}\mathbf{x}, \tag{30}$$

where we have denoted the average pressures on element K by p_K, average traces of the pressures on side E by $\widehat{p}_{K,E}$, and the average density on element K by $\rho_K^{(avg)}$. Denoting

$$B_{E,E'}^K = \int_K (\mathbf{K}^{-1} \mathbf{w}_{K,E}) \cdot \mathbf{w}_{K,E'} \mathrm{d}\mathbf{x}, \quad C_{E'}^K = \int_K \mathbf{g} \cdot \mathbf{w}_{K,E'} \mathrm{d}\mathbf{x}, \tag{31}$$

equation (30) reads as

$$\sum_{E \in \partial K} u_{K,E}(t) B_{E,E'}^K = \lambda_K \left(p_K - \widehat{p}_{K,E'} + \rho_K^{(avg)} C_{E'}^K \right). \tag{32}$$

This equation can be inverted and the velocities $u_{K,E}$ are expressed

$$u_{K,E}(t) = \lambda_K \left(D_E^K p_K - \sum_{E' \partial K} \left(B^K\right)_{E,E'}^{-1} \widehat{p}_{K,E'} + F_E^K \rho_K^{(avg)} \right), \tag{33}$$

where

$$D_E^K = \sum_{E' \in \partial K} \left(B^K\right)_{E,E'}^{-1}, \quad F_E^K = \sum_{E' \in \partial K} \left(B^K\right)_{E,E'}^{-1} C_{E'}^K. \tag{34}$$

Now, we will use continuity assumptions. If side E is not on the boundary, then,

$$u_{K',E} + u_{K,E} = 0, \tag{35}$$

$$\widehat{p}_{K,E} = \widehat{p}_{K',E} =: \widehat{p}_E, \tag{36}$$

where $K' \cap K = E$. If side E is on the boundary, then

$$\widehat{p}_{K,E} = p_E^{(D)}, \text{ for } E \in \Gamma_p, \tag{37}$$

$$u_{K,E} = 0, \text{ for } E \in \Gamma_q. \tag{38}$$

ICCS Camera Ready Version 2021
To cite this paper please use the final published version:
DOI: 10.1007/978-3-030-77980-1_13

Therefore, in equation (33), the velocities $u_{K,E}(t)$ can be eliminated and the only unknowns are $p_K, \widehat{p}_E$. If $E \notin \partial\Omega$, equation (35) implies

$$0 = \sum_{K \supset E} \lambda_K \left(D_E^K p_K - \sum_{E' \in \partial K} \left(B^K\right)^{-1}_{E,E'} \widehat{p}_{E'} + F_E^K \rho_K^{(avg)} \right). \tag{39}$$

On the other hand, if $E \in \partial\Omega$, then

$$\widehat{p}_E = p_E^{(D)}, \text{ if } E \in \Gamma_p, \tag{40}$$

$$-\lambda_K D_E^K p_K + \sum_{E' \in \partial K} \lambda_K \left(B^K\right)^{-1}_{E,E'} \widehat{p}_{E'} = \lambda_K F_E^K \rho_K^{(avg)}, \text{ if } E \in \Gamma_q. \tag{41}$$

Previous equations (39)–(41) form a system of linear equation for the unknowns $\widehat{p}_E, p_K$:

$$\mathbf{R}_1 \mathbf{p} + \mathbf{R}_2 \widehat{\mathbf{p}} = \mathbf{L}_1, \tag{42}$$

where $\mathbf{R}_1 \in \mathbb{R}^{N_{Si}, N_{El}}$, $\mathbf{R}_2 \in \mathbb{R}^{N_{Si}, N_{Si}}$, $\mathbf{L}_1 \in \mathbb{R}^{N_{Si}}$.

3.2 Discretization of pressure equation

Integrating the pressure equation (8) over an element $K \in \tau_\Omega$, and using the divergence theorem results in

$$0 = \phi_K |K| \frac{\mathrm{d}p_K}{\mathrm{d}t} + \sum_{i=1}^{n} \Theta_i \sum_{E \in \partial K} q_{i,K,E} - \sum_{i=1}^{n} \Theta_i \int_K f_i \mathrm{d}\mathbf{x} \tag{43}$$

Using $q_{i,K,E} = \sum_{\alpha=1}^{\Pi} q_{\alpha,i,K,E}$, equation (17), and the backwards Euler scheme, the previous equation can be approximated by

$$\begin{aligned} 0 = \phi_K |K| \frac{p_K^{m+1} - p_K^m}{\Delta t} - \sum_{i=1}^{n} \Theta_i^{m+1} \int_K f_i^{m+1} \mathrm{d}\mathbf{x} + p_K^{m+1} X_K^{m+1} \\ + \sum_{E' \in \partial K} \widehat{p}_{E'}^{m+1} Y_{E'}^{m+1} + Z_K^{m+1}, \end{aligned} \tag{44}$$

where

$$X_K = \sum_{i=1}^{n} \sum_{E \in \partial K} \sum_{\alpha=1}^{\Pi(K)} \Theta_i c_{\alpha,i,K} \lambda_{\alpha,K} D_E^K \tag{45}$$

$$Y_{E'} = \sum_{i=1}^{n} \sum_{E \in \partial K} \sum_{\alpha=1}^{\Pi(K)} -\Theta_i c_{\alpha,i,K} \lambda_{\alpha,K} \left(B_K\right)^{-1}_{E,E'}, \tag{46}$$

$$\begin{aligned} ; Z_K = \sum_{i=1}^{n} \sum_{E \in \partial K} \sum_{\alpha=1}^{\Pi(K)} \lambda_K^{-1} \Theta_i c_{\alpha,i,K} \lambda_{\alpha,K} \Bigg(\lambda_K F_E^K \rho_K^{avg} \\ - \sum_{\beta=1}^{\Pi(K)} \lambda_{\beta,K} (\rho_{\beta,K} - \rho_{\alpha,K}) F_E^K \Bigg), \end{aligned} \tag{47}$$

ICCS Camera Ready Version 2021
To cite this paper please use the final published version:
DOI: 10.1007/978-3-030-77980-1_13

where $c_{\alpha,i,K}$ is the average concentration of the i-th component in phase α on element K. Equation (44) forms a system of linear equation for the unknown p_K^{m+1} and $\widehat{p}_{E'}^{m+1}$

$$\mathbf{R}_3\mathbf{p} + \mathbf{R}_4\widehat{\mathbf{p}} = \mathbf{L}_2, \tag{48}$$

where $\mathbf{R}_3 \in \mathbb{R}^{N_{El},N_{El}}$, $\mathbf{R}_4 \in \mathbb{R}^{N_{El},N_{Si}}$, and $\mathbf{L}_2 \in \mathbb{R}^{N_{El}}$. To conclude, combining equations (42) and (48) gives final system for the pressure field

$$\begin{pmatrix} \mathbf{R}_3 & \mathbf{R}_4 \\ \mathbf{R}_1 & \mathbf{R}_2 \end{pmatrix} \begin{pmatrix} \mathbf{p} \\ \widehat{\mathbf{p}} \end{pmatrix} = \begin{pmatrix} \mathbf{L}_2 \\ \mathbf{L}_1 \end{pmatrix}. \tag{49}$$

The matrix $\mathbf{R}_3$ is diagonal, therefore, its inversion $\mathbf{R}_3^{-1}$ is readily available. Multiplying equation (48) with $\mathbf{R}_3^{-1}$ gives

$$\mathbf{p} = \mathbf{R}_3^{-1}\mathbf{L}_2 - \mathbf{R}_3^{-1}\mathbf{R}_4\widehat{\mathbf{p}} \tag{50}$$

Therefore, the unknowns $\mathbf{p}$ can be eliminated from the system (49), and only the pressure traces $\widehat{\mathbf{p}}$ are computed using

$$(\mathbf{R}_2 - \mathbf{R}_1\mathbf{R}_3^{-1}\mathbf{R}_4)\widehat{\mathbf{p}} = \mathbf{L}_1 - \mathbf{R}_1\mathbf{R}_3^{-1}\mathbf{L}_2. \tag{51}$$

In this work, we use the `C++` numerical library `Armadillo` [20, 21] to solve system (51). Having the pressure traces $\widehat{\mathbf{p}}$, the pressures $\mathbf{p}$ and consequently, the discrete velocities $u_{K,E}$ are computed using equations (50) and (33), respectively.

3.3 Solution of transport equations

Having the pressure field, the concentrations are updated using the explicit finite-volume method. Integrating equation (1) over $K \in \tau_\Omega$, using the divergence theorem, and the Euler scheme results with an approximation of equation (1):

$$c_{i,K}^{m+1} = c_{i,K}^m + \frac{\Delta t}{\phi|K|}\left(|K| f_{i,K}^m - \sum_{E\in\partial K} q_{i,K,E}^m\right), \tag{52}$$

where $c_{i,K}$ and $f_{i,K}$ are the average concentration and source/sink of the i-th component on element K, respectively. The fluxes $q_{i,K,E}$ are calculated using the upwind scheme

$$q_{i,K,E} = \begin{cases} \sum_{\alpha\in\widehat{\Pi^+}(K,E)} q_{\alpha,i,K,E} - \sum_{\beta\in\widehat{\Pi^+}(K,E)} q_{\beta,i,K',E}, & \forall E \notin \partial\Omega, \\ \sum_{\alpha\in\widehat{\Pi^+}(K,E)} q_{\alpha,i,K,E}, & \forall E \in \Gamma_p, \\ 0, \quad \forall E \in \Gamma_q. \end{cases} \tag{53}$$

where $\widehat{\Pi^+}(K,E) = \left\{\alpha \in \widehat{\Pi}(K); q_{\alpha,i,K,E} > 0\right\}$ for $E \in \partial K$ and

$$q_{\alpha,i,K,E} = c_{\alpha,i,K}\lambda_K^{-1}\lambda_{\alpha,K}\left(u_{K,E} - \sum_{\beta=1}^{\Pi(K)} \lambda_{\beta,K}\left(\rho_\beta - \rho_\alpha\right) F_{K,E}\right), \tag{54}$$

where $u_{K,E}$ is given by equation (33).

ICCS Camera Ready Version 2021
To cite this paper please use the final published version:
DOI: 10.1007/978-3-030-77980-1_13

3.4 Algorithm for one time step Δt

Now, we present the full numerical algorithm. This iterative IMPEC algorithm is based on numerical scheme presented in [1]. Having solution on time-level t_m, the solution on time level t_{m+1} is computed using the following algorithm.

1. Set $l = 0$ and $p_K^{m+1,0} = p_K^m, c_{i.K}^{m+1,0} = c_{i,K}^m$, $\Theta_{i,K}^{m+1,0} = \frac{\partial p^{(eq)}}{\partial c_i}\left(c_{1,K}^m, \ldots, c_{n,K}^m\right)$ for $K \in \tau_\Omega, i \in \widehat{n}$.
2. Set $l = l + 1$.
3. On each element $K \in \tau_\Omega$, compute $c_{\alpha,i,K}^{m+1,l-1}$ and $S_{\alpha,K}^{m+1,l-1}$ by solving the phase equilibrium computation given by equations (18)–(19) with initial concentration $c_{1,K}^{m+1,l-1}, \ldots, c_{n,K}^{m+1,l-1}$. In this work, we are using numerical solution presented in [13].
4. On each element $K \in \tau_\Omega$, update $\lambda_K^{m+1,l-1}$ and $\rho_K^{(avg),m+1,l-1}$ using equations (4) and (14) with values $c_{\alpha,i,K}^{m+1,l-1}$ and $S_{\alpha,K}^{n+1,l-1}$ computed in the previous step.
5. Find $p_K^{m+1,l}$ and $u_{K,E}^{m+1,l}$ by solving system (49) with the concentrations $c_{\alpha,i,K}^{m+1,l-1}$, coefficients $\Theta_{i,K}^{m+1,l-1}$, total mobility $\lambda_K^{m+1,l-1}$, and average density $\rho_K^{(avg),m+1,l-1}$.
6. On each element $K \in \tau_\Omega$, for all $i \in \widehat{n}$ update $c_{i,K}^{m+1,l}$ explicitly by

$$c_{i,K}^{m+1,l} = c_{i,K}^m + \frac{\Delta t}{\phi |K|}\left(|K| f_{i,K}^m - \sum_{E \in \partial K} q_{i,K,E}^{m+1,l-1}\right), \tag{55}$$

   where the flux $q_{i,K,E}^{m+1,l-1}$ is evaluated using the velocity $u_{K,E}^{m+1,l}$ and concentrations $c_{\alpha,i,K}^{m+1,l-1}$.
7. On each element $K \in \tau_\Omega$, for all $i \in \widehat{n}$ update $\Theta_{i,K}^{m+1,l}$ by

$$\Theta_{i,K}^{m+1,l} = \frac{p^{(eq)}(\mathbf{c}^{(1)}) - p^{(eq)}(\mathbf{c}^{(2)})}{c_{i,K}^{m+1,l} - c_{i,K}^m}, \tag{56}$$

   where

$$\mathbf{c}^{(1)} = \left(c_{1,K}^{m+1,l}, \ldots, c_{i,K}^{m+1,l}, c_{i+1,K}^m, \ldots, c_{n,K}^m\right)^T, \tag{57}$$

$$\mathbf{c}^{(2)} = \left(c_{1,K}^{m+1,l}, \ldots, c_{i-1,K}^{m+1,l}, c_{i,K}^m, \ldots, c_{n,K}^m\right)^T. \tag{58}$$

   To compute the pressures, the phase equilibrium computation is used to determine the number of phases and the equilibrium pressure.
8. Check convergence. If the convergence criteria are met, set

$$p_K^{m+1} = p_K^{m+1,l}, \quad c_{i,K}^{m+1} = c_{i,K}^{m+1,l}, \quad \forall K \in \tau_\Omega, \forall i \in \widehat{n}, \tag{59}$$

ICCS Camera Ready Version 2021
To cite this paper please use the final published version:
DOI: 10.1007/978-3-030-77980-1_13

and terminate the Algorithm. Otherwise, go to step 2. In this work, we terminate the algorithm if the maximum number of iterations $l_{\max}$ is reached or the criterion

$$\max\left\{\frac{\left\|p^{m+1,l}-p^{m+1,l-1}\right\|}{\left\|p^{m+1,l}\right\|},\sum_{i=1}^{n}\frac{\left\|c_i^{m+1,l}-c_i^{m+1,l-1}\right\|}{\left\|c_i^{m+1,l}\right\|},\sum_{i=1}^{n}\frac{\left\|\Theta_i^{m+1,l}-\Theta_i^{m+1,l-1}\right\|}{\left\|\Theta_i^{m+1,l}\right\|}\right\}<\varepsilon, \tag{60}$$

is fullfilled. In previous equation $\|\cdot\|$ is the $L^2(\Omega)$ norm and ε is a given tolerance.

4 Numerical results

In this section, we provide two numerical examples. In both examples, the computation domain Ω is a square domain of size 50×50 meters with porosity $\phi = 0.2$ and isotropic permeability $\mathbf{K} = k = 9.87 \times 10^{-15}$ m^2, i.e., 10 mD. Moreover, we use a triangular mesh with $2 \times 20 \times 20$ elements, i.e., total 400 elements are used. The final time in both examples is $t_{\text{final}} = 150$ days. The ε tolerance is set to $\varepsilon = 10^{-8}$, and the maximum number of inner iterations is set to $l_{\max} = 30$. For the computation, a computer with Intel(R) Core(TM) i7-8700 (3.20GHz) processor was used.

4.1 Example 1: C_1 injection

In the first example, we simulate the injection of methane (C_1) into a horizontal (i.e., no gravity) reservoir. The reservoir is initially filled with with a mixture of 95 % propane and 5 % methane at a constant pressure $p = 6.9$ MPa and temperature $T = 311$ K. The mixture with 95 % of the methane is injected at the right bottom corner. The rate of the injection is 125.33 m^2 per day at atmospheric pressure and temperature 293 K. In Table 1, the parameters for the Peng-Robinson equation of state are presented. The binary interaction coefficient is $\delta_{C_1-C_3} = 0.0365$. The boundary of the domain is impermeable except for the outflow corner where pressure $p = 6.9$ MPa is maintained. The time step was set to $\Delta t = 3000$ seconds. In Figure 1, the iso-lines of methane mole fraction at different times are depicted. The values are from 0.05 to 0.95 with a step size 0.1. Moreover, in Figure 1, the two-phase region is depicted in the black color. The total computation time was 2.5 hours.

4.2 Example 2: CO_2 injection

In the second example, we simulate the injection of carbon dioxide (CO_2) into a vertical (i.e., with gravity) reservoir. The reservoir is initially filled with pure

ICCS Camera Ready Version 2021
To cite this paper please use the final published version:
DOI: 10.1007/978-3-030-77980-1_13

propane at a constant pressure $p = 5$ MPa and temperature $T = 311$ K. The CO_2 is injected at the right bottom corner. The rate of the injection is 125.33 m^2 per day at atmospheric pressure and temperature 293 K. In Table 1, the parameters for the Peng-Robinson equation of state are presented. The binary interaction coefficient is $\delta_{C_1-C_3} = 0.15$. The boundary of the domain is impermeable except for the outflow corner where pressure $p = 5$ MPa is maintained. To reach convergence, the time step had to be decreased to $\Delta t = 500$ seconds and the maximum number of iteration increased to $l_{\max} = 50$. In Figure 2, the iso-lines of carbon dioxide mole fraction at different times are depicted. The values are from 0.05 to 0.95 with step size 0.1. Moreover, in Figure 2, the two-phase region is depicted in the black color. The total computation time was approximately 24 hours.

component	T_{crit} [K]	P_{crit} [MPa]	ω [-]	M [g mol^{-1}]	V_{crit} [m^3 kg^{-1}]
C_1	190.56	4.599	0.011	16.0	6.10639×10^{-3}
C_3	369.83	4.248	0.153	44.096	4.53554×10^{-3}
CO_2	304.14	7.375	0.239	44.0	2.13589×10^{-3}

Table 1. Component properties.

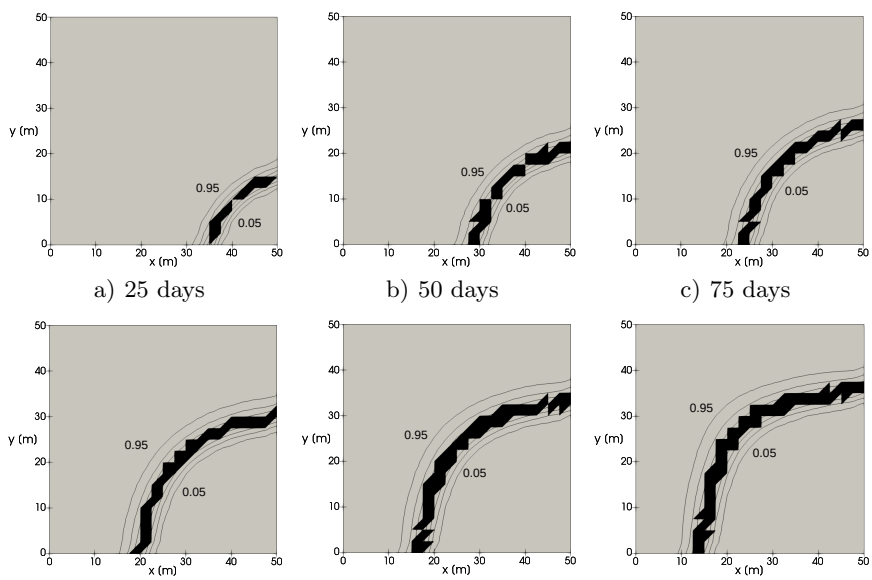

a) 25 days b) 50 days c) 75 days

d) 100 days e) 125 days f) 150 days

Fig. 1. The iso-lines of methane mole fraction in different times. The values are from 0.05 to 0.95 with step size 0.1. The two-phase area is depicted in the black color. Example 1: C_1 injection.

ICCS Camera Ready Version 2021
To cite this paper please use the final published version:
DOI: 10.1007/978-3-030-77980-1_13

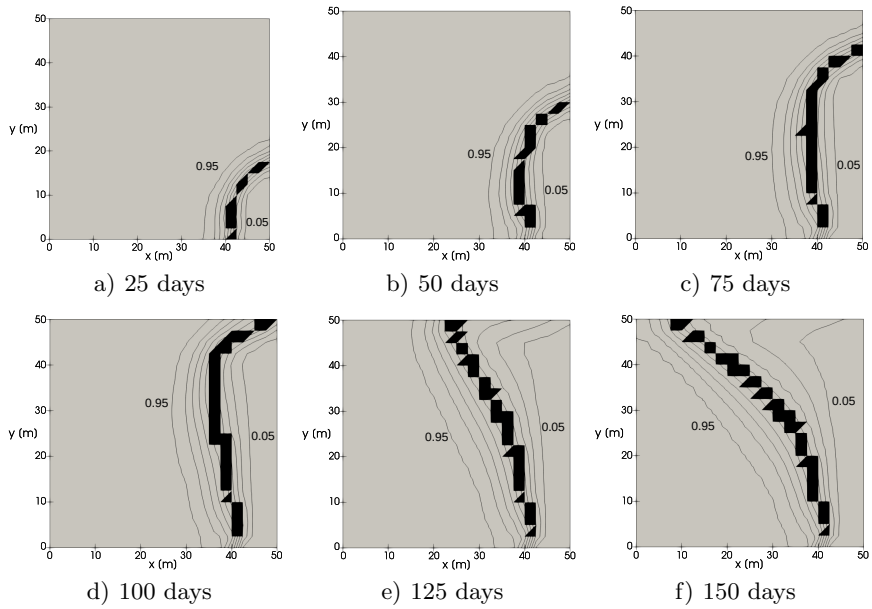

a) 25 days b) 50 days c) 75 days

d) 100 days e) 125 days f) 150 days

Fig. 2. The iso-lines of carbon dioxide mole fraction in different times. The values are from 0.05 to 0.95 with step size 0.1. The two-phase area is depicted in the black color. Example 2: CO_2 injection.

5 Conclusion

In this paper, we presented a new numerical solution of multi-phase compositional flow in a porous medium. The numerical solution is based on mixed-hybrid finite element method and a novel iterative IMPEC scheme. Unlike in tradition solvers, the local thermodynamical behaviour is determined by the phase equilibrium computation in the VTN-specification. Using this specification, unpleasant properties such as non-uniqueness of the equilibrium states are avoided. We provided two examples showing the performance of the numerical scheme. In the second example, the time step has to be significantly decreased to reach convergence. Investigation of this phenomenon is our current research.

References

1. H. Chen, X. Fan, and S. Sun, "A fully mass-conservative iterative IMPEC method for multicomponent compressible flow in porous media," *Journal of Computational and Applied Mathematics*, vol. 362, pp. 1 – 21, 2019.
2. G. Acs, S. Doleschall, and E. Farkas, "General purpose compositional model," *Society of Petroleum Engineers*, vol. 25, pp. 543–553, 1985.

ICCS Camera Ready Version 2021
To cite this paper please use the final published version:
DOI: 10.1007/978-3-030-77980-1_13

3. L. C. Young and R. E. Stephenson, "A generalized compositional approach for reservoir simulation," *Society of Petroleum Engineers Journal*, vol. 23, pp. 727–742, 1983.
4. M. L. Michelsen, "The isothermal flash problem, part 2. Phase-split computation," *Fluid Phase Equilibria*, vol. 9, pp. 21–40, 1982.
5. Z. Li and A. Firoozabadi, "General strategy for stability testing and phase-split calculation in two and three phases," *Society of Petroleum Engineers*, vol. 17, pp. 1096–1107, 2012.
6. J. Mikyška and A. Firoozabadi, "Investigation of mixture stability at given volume, temperature, and moles," *Fluid Phase Equilibria*, vol. 321, pp. 1–9, 2012.
7. O. Polívka and J. Mikyška, "Compositional modeling in porous media using constant volume flash and flux computation without the need for phase identification," *Journal of Computational Physics*, vol. 272, pp. 149–179, 2014.
8. T. Jindrová and J. Mikyška, "General algorithm for multiphase equilibria calculation at given volume, temperature, and moles," *Fluid Phase Equilibria*, vol. 393, pp. 7–25, 2015.
9. M. Castier, "Helmholtz function-based global phase stability test and its link to the isothermal-isochoric flash problem," *Fluid Phase Equilibria*, vol. 379, pp. 104–111, 2014.
10. S. Sun, A. Firoozabadi, and J. Kou, "Numerical modeling of two-phase binary fluid mixing using mixed finite elements," *Computational Geosciences*, vol. 16, pp. 1101–1124, 2012.
11. H. Hoteit and A. Firoozabadi, "Compositional modeling by the combined discontinuous Galerkin and mixed methods," *Society of Petroleum Engineers*, vol. 11, pp. 19–34, 2006.
12. A. Zidane and A. Firoozabadi, "Two-phase compositional flow simulation in complex fractured media by 3D unstructured gridding with horizontal and deviated wells," *SPE Reservoir Evaluation & Engineering*, vol. 23, 12 2019.
13. T. Smejkal and J. Mikyška, "Unified presentation and comparison of various formulations of the phase stability and phase equilibrium calculation problems," *Fluid Phase Equilibria*, vol. 476, pp. 61–88, 2018.
14. J. Lohrenz, B. G. Bray, and C. R. Clark, "Calculating viscosities of reservoir fluids from their compositions," *Journal of Petroleum Technology*, vol. 16, no. 10, pp. 1171–1176, 1964.
15. A. Firoozabadi, *Thermodynamics and Applications of Hydrocarbons Energy Production*. McGrew-Hill, 2015.
16. T. Smejkal and J. Mikyška, "Efficient solution of linear systems arising in the linearization of the VTN-phase stability problem using the Sherman-Morrison iterations," *Fluid Phase Equilibria*, vol. 527, p. 112832, 2021.
17. D.-Y. Peng and D. B. Robinson, "A new two-constant equation of state," *Industrial & Engineering Chemistry Fundamentals*, vol. 15, pp. 59–64, Feb. 1976.
18. F. Brezzi and M. Fortin, *Mixed and hybrid finite element methods*, vol. 15. Springer Science & Business Media, 2012.
19. P.-A. Raviart and J. Thomas, *Mathematical Aspects of Finite Element Methods*. Springer, 1977.
20. D. Eddelbuettel and C. Sanderson, "RcppArmadillo: Accelerating R with high-performance C++ linear algebra," *Computational Statistics and Data Analysis*, vol. 71, pp. 1054–1063, March 2014.
21. C. Sanderson and R. Curtin, "Armadillo: a template-based C++ library for linear algebra," *Journal of Open Source Software*, vol. 1, no. 2, p. 26, 2016.

ICCS Camera Ready Version 2021
To cite this paper please use the final published version:
DOI: 10.1007/978-3-030-77980-1_13